Molecular engineering of polymeric carbon nitride for photocatalytic hydrogen production with ultrahigh apparent quantum efficiency

*Haiyang Liu,[a,1] Xiaolu Liu,[b,1] Chengqun Xu,[*ad] Dongyu Wang,[a] Dezhi Li,[a] Jingyao Huang,[a] Shengquan Wu,[a] Zhichun Wang,[a] and Hui Pan [*b,c]*

[a]School of Applied Physics and Materials, Wuyi University, Jiangmen 529020, P. R. China. E-mail: xuchengqun2019@yeah.net

[b]Institute of Applied Physics and Materials Engineering, University of Macau, Macao SAR, 999078, P. R. China. Email: huipan@um.edu.mo

[c]Department of Physics and Chemistry, Faculty of Science and Technology, University of Macau, Macao SAR, 999078, P. R. China

[d]International Center for Materials Nanoarchitectonics (WPI-MANA), National Institute for Materials Science (NIMS), 1-1 Namiki, Tsukuba, Ibaraki 305-0044, Japan.

Computational details:

Band structures of MCN and MCN-*x*TAP-NaK were computed based on the density functional theory (DFT). The Perdew-Burke-Ernzerhof (PBE) functional and plane-wave ultrasoft pseudopotential implemented in the CASTEP code were used [1, 2]. This level of theory has been widely tested and afforded reasonable results on the electronic structures and energetics for C_3N_4 and its derivatives [3, 4]. Because the weak interactions are not well described by the standard PBE functional, the DFT-D approach within the Grimme scheme was adopted for the vdW corrections [5]. A 340 eV energy cutoff and a 3 × 3 × 1 k-point mesh were used. The convergence tolerance of energy was taken as 10^{-5} eV/atom, and the maximum allowed force and displacement were set as 0.03 eV/Å and 0.001 Å, respectively. A large vacuum space of 15 Å in the z direction was applied to eliminate the interactions between neighboring layers.

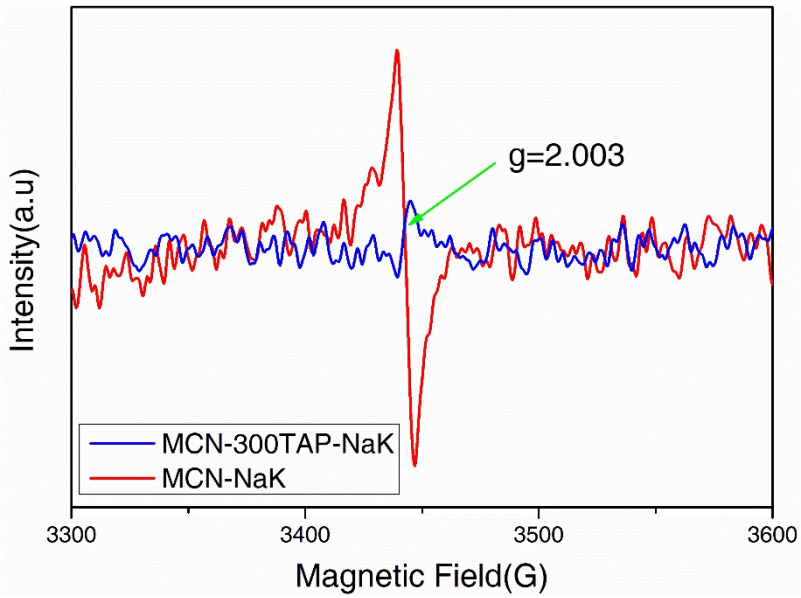

Figure S1. EPR spectra of MCN-NaK and MCN-300TAP-NaK in the dark.

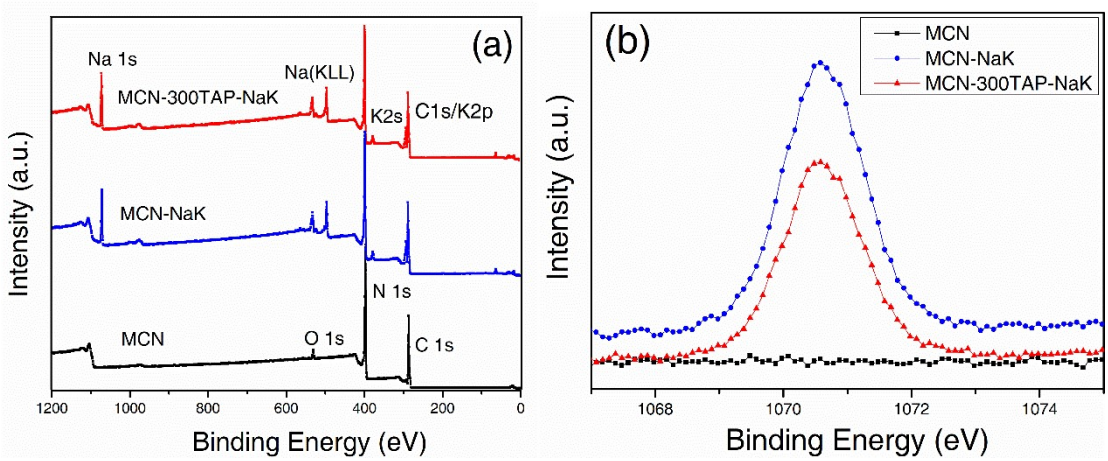

Figure S2. X-ray photoelectron spectra of MCN, MCN-NaK and MCN-300TAP-NaK: (a) survey and (b) Na 1s.

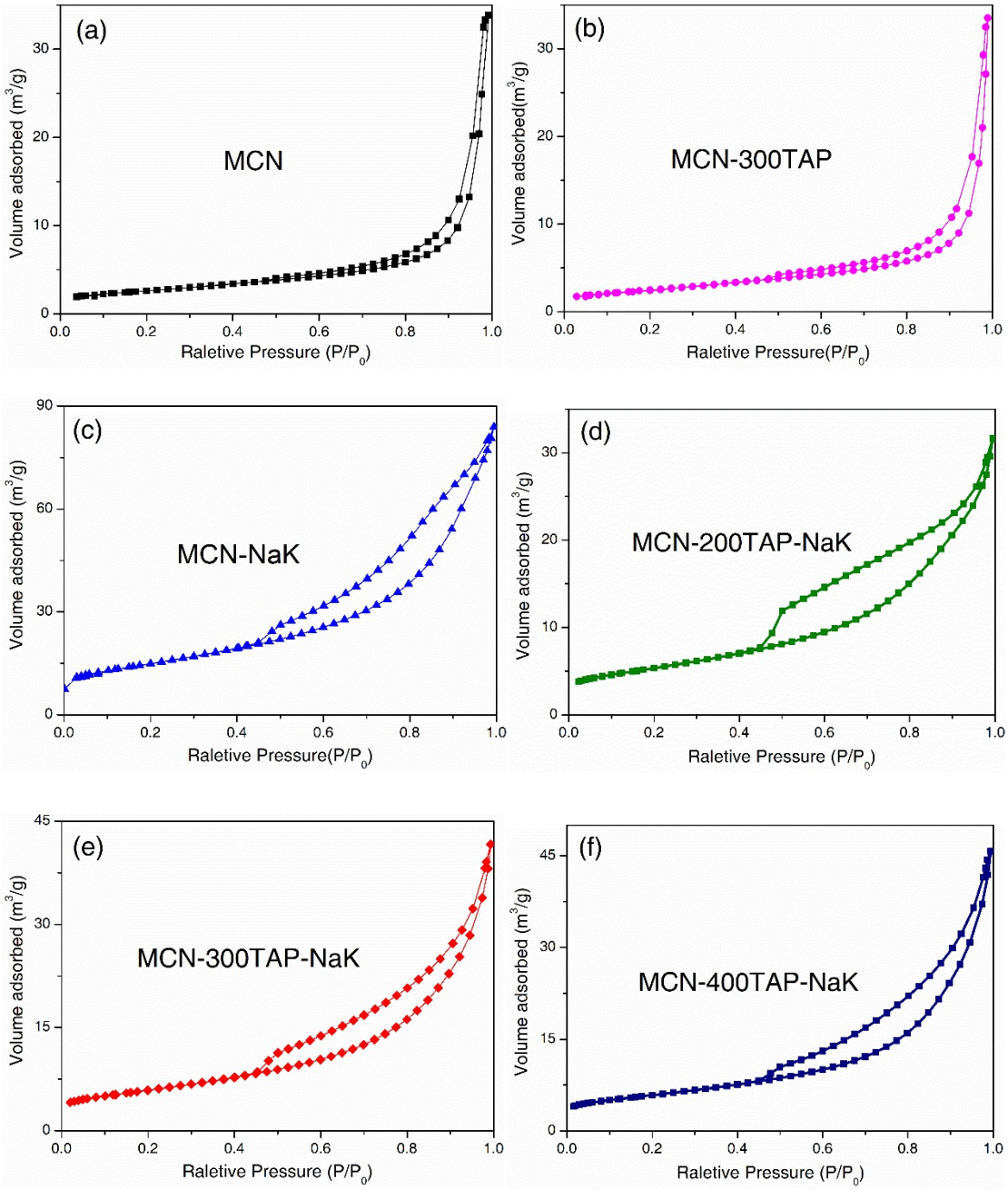

Figure S3. N_2 adsorption/desorption isotherms of MCN, MCN-NaK and MCN-*x*TAP-NaK.

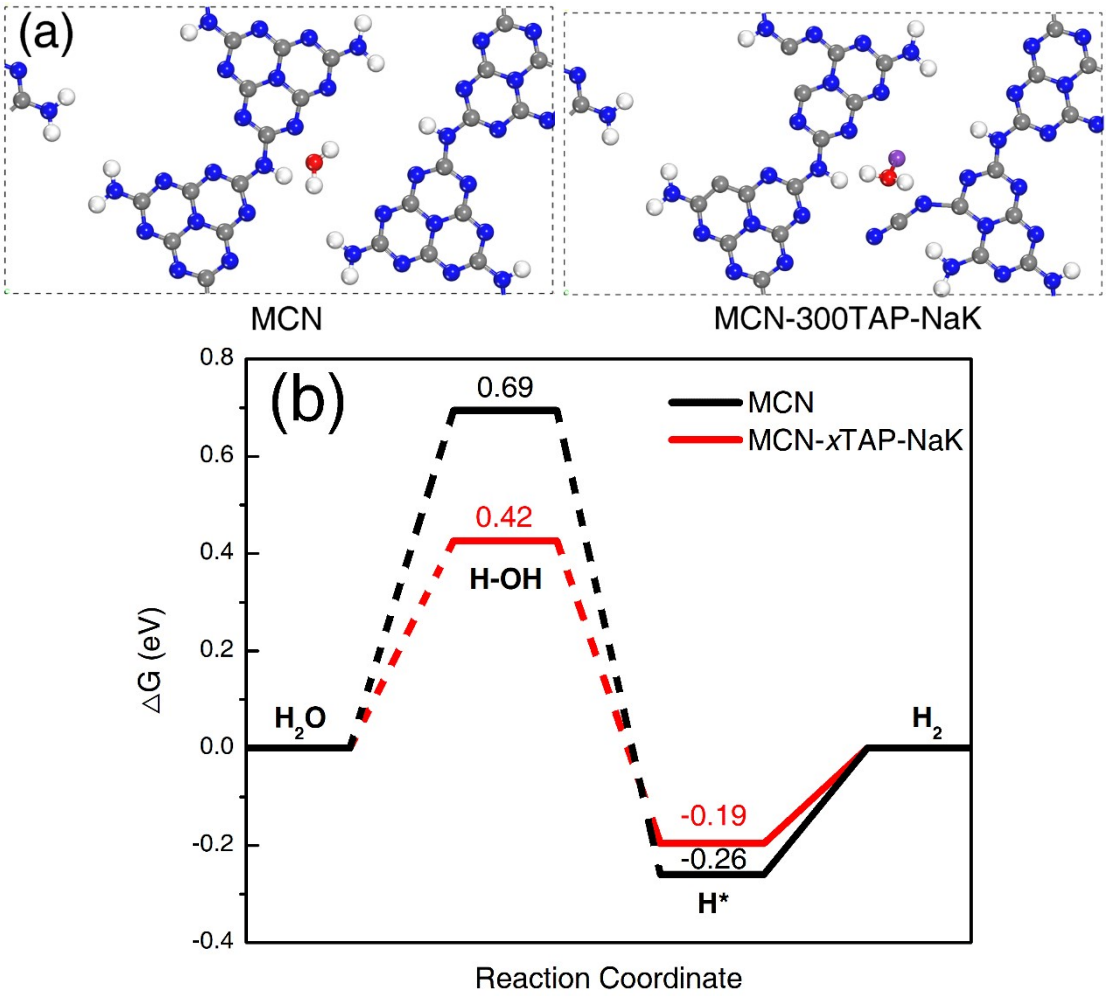

Figure S4. (a) Water adsorption models on the surface of MCN and MCN-*x*TAP-NaK; (b) Free energy diagrams for H_2O reduction to H_2 by the thermochemical model on MCN and MCN-*x*TAP-NaK.

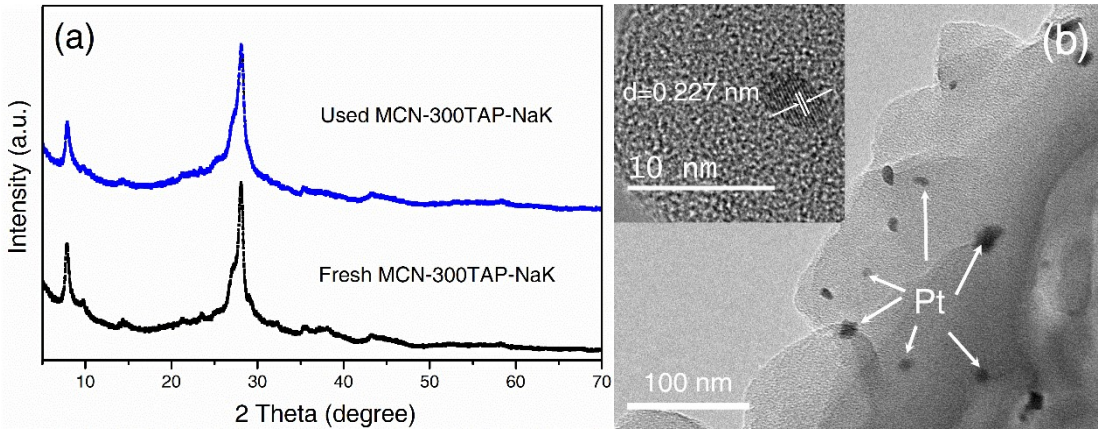

Figure S5. (a) XRD patterns and (b) HR-TEM image of MCN-300TAP-NaK after photocatalytic H_2 evolution.

Table S1. EIS fitted parameters of MCN, MCN-NaK and MCN-*x*TAP-NaK. The equivalent circuits consist of series resistance (R_s), the charge tranfer resistance (R_{ct}) and the constant phase element (CPE1).

	MCN	MCN-300TAP	MCN-NaK	MCN-200TAP-NaK	MCN-300TAP-NaK	MCN-400TAP-NaK
R_s (Ω)	324.9	310.1	316.4	301.2	301.9	297.1
R_{ct} (Ω)	167150	98567	74934	59372	42269	46989
CPE1 (F)*10^{-5}	1.04	1.03	1.16	1.09	1.06	1.12

Table S2. AQE values of the as-prepared samples in the presence of different molten salts under a series of monochromatic light irradiations.

Samples	$AQE_{450\ nm}$	$AQE_{500\ nm}$	$AQE_{550\ nm}$	$AQE_{600\ nm}$	$AQE_{650\ nm}$
MCN-300TAP-NaK (no salts)	14.2%	12.0%	4.4%	0.8%	0.3%
MCN-300TAP-NaK (NaCl)	59.8%	21.5%	8.0%	0.7%	0.4%
MCN-300TAP-NaK (K_2HPO_4)	77.8%	29.4%	12.1%	1.8%	0.5%
MCN-300TAP-NaK (KCl)	46.2%	17.5%	4.7%	0.4%	0.2%
MCN (no salts)	0.9%	0	0	0	0

Table S3. Comparison of photocatalytic activity of the reported g-C_3N_4.

Catalyst	Light Source	Reaction Conditions	Apparent quantum efficiency	Ref.
MCN-300TAP-NaK (K_2HPO_4)	300 W Xe lamp	3 wt% of Pt; Aqueous TEOA solution (10 vol%)	77.8% (450 nm) 29.4% (500 nm) 12.1% (550 nm) 1.8% (600 nm)	This work
CN-ATZ-NaK (K_2HPO_4)	50 W While LED light	3 wt% of Pt; Aqueous MeOH solution (10 vol%)	65% (420 nm)	[6]
g-C_3N_4 nanosheet (K_2HPO_4)	300 W Xe lamp	3 wt% of Pt; Aqueous TEOA solution (10 vol%)	45.7% (380 nm) 26.1% (420 nm)	[7]
CN-NaK (NaCl)	50 W While LED light	3 wt% of Pt; Aqueous TEOA solution (10 vol%)	60% (420 nm)	[8]
CN-m (NaCl)	50 W While LED light	3 wt% of Pt; Aqueous TEOA solution (10 vol%)	57% (420 nm)	[9]
g-CN-1 (K_2HPO_4)	300 W Xe lamp	3 wt% of Pt; Aqueous TEOA solution (10 vol%)	50.7% (405 nm)	[10]
UCN-5TDA	300 W Xe lamp	3 wt% of Pt; Aqueous TEOA solution (10 vol%)	13.3% (450 nm) 7.93% (500 nm) 1.25% (550 nm)	[11]
UCN-BI_{400}	300 W Xe lamp, $\lambda > 420$ nm	3 wt% of Pt; Aqueous TEOA solution (20 vol%)	7% (450 nm) 3% (500 nm) 0.5% (550 nm)	[12]
UCN-4TAPB	300 W Xe lamp, $\lambda > 420$ nm	3 wt% of Pt; Aqueous TEOA solution (10 vol%)	40.0% (400 nm) 3.8% (500 nm)	[13]
PTI-0.13	300 W Xe lamp	3 wt% of Pt; Aqueous TEOA solution (10 vol%)	7.0% (420 nm) 4.6% (450 nm) 0.8% (550 nm)	[14]
O-CN2	300 W Xe lamp	1 wt% of Pt; Aqueous Lactic acid solution (10 vol%)	13.2% (420 nm) 4.5% (450 nm) 1.5% (500 nm) 1.0% (550 nm)	[15]
UM3	300 W Xe lamp	1 wt% of Pt; Aqueous Lactic acid solution (20 vol%)	27.8% (420 nm) 12% (450 nm) 7% (500 nm)	[16]
g-C_3N_4 (urea)	300 W Xe lamp	3 wt% of Pt; Aqueous TEOA	26.5% (400 nm) 12.5% (420 nm)	[17]

	solution (13 vol%)	4% (450 nm)

Reference:

[1] M. Segall, P.J. Lindan, M.a. Probert, C.J. Pickard, P.J. Hasnip, S. Clark, M. Payne, J. Phys: Condens. Mat. 14 (2002) 2717.
[2] J.P. Perdew, K. Burke, M. Ernzerhof, Phys. Rev. Lett. 77 (1996) 3865.
[3] S. Shi, M. Gondal, S. Rashid, Q. Qi, A. Al Saadi, Z. Yamani, Y. Sui, Q. Xu, K. Shen, Colloid. Surface. A. 461 (2014) 202-211.
[4] B. Zhu, J. Zhang, C. Jiang, B. Cheng, J. Yu, Appl. Catal. B: Environ 207 (2017) 27-34.
[5] S. Grimme, J. Comput. Chem. 27 (2006) 1787-1799.
[6] G. Zhang, G. Li, T. Heil, S. Zafeiratos, F. Lai, A. Savateev, M. Antonietti, X. Wang, Angewandte Chemie International Edition 58 (2019) 3433-3437.
[7] G. Liu, T. Wang, H. Zhang, X. Meng, D. Hao, K. Chang, P. Li, T. Kako, J. Ye, Angewandte Chemie International Edition 54 (2015) 13561-13565.
[8] G. Zhang, L. Lin, G. Li, Y. Zhang, A. Savateev, S. Zafeiratos, X. Wang, M. Antonietti, Angewandte Chemie International Edition 130 (2018) 9516-9520.
[9] G. Zhang, G. Li, Z. Lan, L. Lin, A. Savateev, T. Heil, S. Zafeiratos, X. Wang, M. Antonietti, Angewandte Chemie International Edition 129 (2017) 13630-13634.
[10] L. Lin, H. Ou, Y. Zhang, X. Wang, ACS Catalysis 6 (2016) 3921-3931.
[11] C. Xu, X. Liu, H. Liu, D. Li, Y. Yang, S. Lin, D. Fan, H. Pan, Journal of Materials Chemistry A 10 (2022) 21031-21043.
[12] H. Che, C. Li, C. Li, C. Liu, H. Dong, X. Song, Chemical Engineering Journal 410 (2021) 127791.
[13] C. Xu, X. Liu, D. Li, Z. Chen, J. Yang, J. Huang, H. Pan, ACS Applied Materials & Interfaces 13 (2021) 20114-20124.
[14] M.K. Bhunia, K. Yamauchi, K. Takanabe, Angewandte Chemie International Edition 53 (2014) 11001-11005.
[15] C. Liu, H. Huang, W. Cui, F. Dong, Y. Zhang, Applied Catalysis B: Environmental 230 (2018) 115-124.
[16] N. Tian, Y. Zhang, X. Li, K. Xiao, X. Du, F. Dong, G.I. Waterhouse, T. Zhang, H. Huang, Nano Energy 38 (2017) 72-81.
[17] D.J. Martin, K. Qiu, S.A. Shevlin, A.D. Handoko, X. Chen, Z. Guo, J. Tang, Angewandte Chemie International Edition 53 (2014) 9240-9245.